

Noise-based reward-modulated learning

Jesús García Fernández¹, Nasir Ahmad¹, and Marcel van Gerven¹

¹Department of Machine Learning and Neural Computing, Donders Institute for Brain, Cognition and Behaviour, Radboud University, Nijmegen, the Netherlands

Abstract

Recent advances in reinforcement learning (RL) have led to significant improvements in task performance. However, training neural networks in an RL regime is typically achieved in combination with backpropagation, limiting their applicability in resource-constrained environments or when using non-differentiable neural networks. While noise-based alternatives like reward-modulated Hebbian learning (RMHL) have been proposed, their performance has remained limited, especially in scenarios with delayed rewards, which require retrospective credit assignment over time. Here, we derive a novel noise-based learning rule that addresses these challenges. Our approach combines directional derivative theory with Hebbian-like updates to enable efficient, gradient-free learning in RL. It features stochastic noisy neurons which can approximate gradients, and produces local synaptic updates modulated by a global reward signal. Drawing on concepts from neuroscience, our method uses reward prediction error as its optimization target to generate increasingly advantageous behavior, and incorporates an eligibility trace to facilitate temporal credit assignment in environments with delayed rewards. Its formulation relies on local information alone, making it compatible with implementations in neuromorphic hardware. Experimental validation shows that our approach significantly outperforms RMHL and is competitive with BP-based baselines, highlighting the promise of noise-based, biologically inspired learning for low-power and real-time applications.

1 Introduction

Noise-based learning methods, which leverage stochastic fluctuations in neural activity [15, 20, 54, 52, 13] or synaptic weights [10, 57, 5, 8] to approximate gradients, offer a pathway toward simpler and more light-weight optimization techniques, that may reflect mechanisms within the brain itself [43, 29]. Given the prevalence of noise in biological neural systems [9, 45, 31], using noise as a mechanism for learning synaptic weights is an area of growing interest, with reward-modulated Hebbian learning (RMHL) [26, 32] as a promising candidate. RMHL, a form of three-factor Hebbian learning [17, 24], offers a potentially powerful mechanism for credit assignment without explicit backpropagation of exact gradients.

Despite theoretical advances, few noise-based methods have been adapted to real-world tasks. Some attempts which have been made include application to control problems [4], for spatiotemporal pattern generation [23], and for training non-differentiable spiking neural networks training [12], and these particularly struggle with delayed reward regimes. This gap has limited the integration of noise-based approaches for effective credit assignment in temporally extended setups.

In this work, we address this gap by proposing a novel noise-driven learning mechanism for reinforcement learning (RL), referred to as noise-based reward-modulated learning (NRL), which leverages noise to approximate gradients for synaptic updates derived from reward maximization. NRL integrates key concepts from neuroscience, such as eligibility traces [19], which link past neural states to future rewards, and reward prediction error (RPE) [41, 40, 34], which drives learning toward increasingly more advantageous behaviors. We employ directional derivatives for gradient approximation, which is realized through stochastic neurons that are compatible with the inherently noisy nature of brains and other physical systems. NRL estimates the directional derivative via two forward passes: a “noisy” pass with stochastic neurons and a “clean” pass without noise. In scenarios where a noiseless pass is infeasible, as in noisy analog hardware, multiple noisy passes can be averaged to approximate the clean pass, maintaining performance. We further validate our approach on RL benchmarks

with both immediate- and delayed-reward problems. Finally, we discuss the broader implications for machine learning, neuromorphic computing, and neuroscience.

2 Methods

2.1 Agent-environment setup and learning signals

We consider an agent interacting continuously with a dynamic environment, whose state at time t is denoted by S_t . The agent observes S_t and responds by selecting actions, A_t , which influence the environment. Each action or sequence of actions yields feedback in the form of positive or negative rewards r_t . This observe-act loop provides a feedback loop which can be leveraged to enable an agent to learn and adapt to the changing environment, aiming to maximize the rewards associated with its actions.

The agent’s decision-making is guided by a policy π , representing the probability of choosing an action, a , in the state S_t , i.e., $\pi(a | S_t)$. This policy reflects the agent’s understanding of optimal actions in each state. To determine an action, the agent computes a probability distribution over the set of possible actions, modeled as a categorical distribution, where $\sum_a \pi(a | S_t) = 1$, such that

$$P(A_t = a | S_t) = \pi(a | S_t). \quad (1)$$

Rewards, r_t , from the environment, received after each action or sequence of actions, are used to compute the learning signal. Internally, the agent maintains a prediction of reward, denoted by \bar{r}_t . This prediction could be formed by an arbitrary computation, but for simplicity it is modeled as a running average over recent rewards

$$\bar{r}_t = \bar{r}_{t-1} + \lambda(r_t - \bar{r}_{t-1}) \quad (2)$$

where λ is a smoothing factor. The mismatch between the predicted reward and the actual reward, denoted by

$$\delta r_t = r_t - \bar{r}_t \quad (3)$$

serves as the primary learning signal. It can be interpreted as a reward prediction error (RPE) in neuroscience contexts and can be thought of as a global dopaminergic signal that modulates learning in the brain [41, 40, 34]. While conceptually similar to biological RPEs, this formulation is a simplification due to the straightforward running average used for reward prediction. Nonetheless, it effectively captures the core ideas of the proposed learning mechanism. In the Discussion, we explore how this prediction error could be refined.

2.2 Derivation of the learning rule

This section presents a complete derivation of the NRL update rule. We begin by establishing a gradient-based learning rule rooted in an optimization target that aims to maximize unexpected rewards from the environment by increasing the reward prediction error. Maximizing the RPE rather than the direct reward enables the agent to adapt dynamically to changing environments, improve long-term performance by continuously seeking rewards that exceed expectations, and maintain robustness against variations in reward structures [48, 36]. Building on this foundation, we transition to a gradient-free formulation by leveraging a directional derivative framework, where stochastic noise within the network approximates gradients. This eliminates the need for explicit backpropagation and feedback phases, enabling learning through forward passes alone. Finally, we extend our noise-based approach to handle scenarios with delayed rewards, a hallmark of real-world problems. This extension enables NRL to adapt to environments where feedback is only obtained after a series of actions.

2.2.1 Gradient-based learning rule

The agent is represented by a neural network which processes input observations and generates a probability distribution over possible actions. This neural network consists of multiple layers, each performing a linear transformation of its inputs, followed by a non-linear transformation as

$$x^l = f(h^l) = f(W^l x^{l-1}) \quad (4)$$

where x^l represents the output of layer l , h^l represents the layer pre-activation, W^l is the weight matrix, and $f(\cdot)$ is a non-linear activation function.

In this setup, the goal is to optimize the weights $W = \{W^1, \dots, W^L\}$ across the L layers in the neural network to maximize the received rewards. Our derivation begins by introducing a generic variable θ , which will later be mapped to the specific neural network parameters W . The primary learning objective is to maximize the expected RPE, δr_t , which aims to achieve higher-than-anticipated rewards. For now, let us consider learning to maximise RPE at a specific timepoint t . Since the reward prediction is a running average of recent rewards, the learning rule seeks to outperform previously received rewards. We express this objective in terms of the policy as

$$J(\theta) = \mathbb{E}_{\pi_\theta} [\delta r_t] . \quad (5)$$

To optimize $J(\theta)$, we can incrementally update the weights using the gradients with respect to θ as

$$\theta \leftarrow \theta + \eta \nabla_\theta J(\theta) \quad (6)$$

where η is the learning rate, controlling the size of each update step.

Applying the policy gradient theorem [49], which utilizes the likelihood-ratio method, we express the gradient of the objective as

$$\nabla_\theta J(\theta) = \mathbb{E}_{\pi_\theta} [\nabla_\theta \log \pi_\theta (a | S_t) \delta r_t] . \quad (7)$$

For empirical estimation, in the case of a single sample, we approximate the gradient as

$$\nabla_\theta J(\theta) \approx \nabla_\theta \log \pi_\theta (a | S_t) \delta r_t . \quad (8)$$

With this approximation, we define the parameter updates as

$$\theta \leftarrow \theta + \eta \nabla_\theta \log \pi_\theta (a | S_t) \delta r_t . \quad (9)$$

Equation (9) resembles the REINFORCE update rule [54] but differs by using the reward prediction error (RPE), δr_t , as the learning signal instead of cumulative rewards over full trajectories. This RPE-based approach leverages immediate feedback from rewards as they are obtained rather than requiring a full trial completion to estimate the policy gradient. It shares conceptual similarities with actor-critic methods [1], where the policy is adjusted using a temporal difference error. However, we approximate future rewards with a running average of past rewards instead of a critic network, maintaining adaptive feedback benefits with a simpler implementation.

2.2.2 Noise-based learning rule

The learning rule derived in the previous section still relies on gradient descent. To avoid using backpropagation (BP) to compute the gradients, we propose a noise-based alternative that extends Equation (9). This approach leverages gradient approximation via directional derivatives, as detailed in Appendix A, enabling a theoretically rigorous derivation of noise-driven learning.

A directional derivative quantifies the rate of change of a function in a specified direction. In neural networks, we implement this concept by introducing random noise into parameters. By comparing the network's parameters with and without this noise, we obtain an estimate of the gradient direction. To formalize this, we express the gradient term in terms of directional derivatives using Theorem A.3 in Appendix A as

$$\nabla p(\theta) = \nabla_\theta \log \pi_\theta(a | S_t) = n \mathbb{E} [v \nabla_v p(\theta)] \quad (10)$$

where $v = \epsilon / \|\epsilon\|$ is a normalized direction vector derived from noise $\epsilon \sim \mathcal{N}(0, \sigma^2 I_n)$ with n the number of parameters.

We may expand the above via Theorem A.4, and add a difference term (parameters with noise versus without noise) to approximate the gradient by sampling under an empirical distribution

$$\nabla p(\theta) = n \sum_{i=1}^K \left[\frac{\epsilon^{(i)}}{\|\epsilon^{(i)}\|^2} \left(p(\tilde{\theta}^{(i)}) - p(\theta) \right) \right] . \quad (11)$$

where K denotes the number of samples and $\tilde{\theta}^{(i)} = \theta + \epsilon^{(i)}$ the noise-perturbed parameters. In practice, we consider $K = 1$, analogous to single-sample updates in stochastic gradient descent. Here, $p(\tilde{\theta}) = \log \pi_{\tilde{\theta}}(a | S_t)$ represents the log of the noise-perturbed output, while, $p(\theta) = \log \pi_{\theta}(a | S_t)$ is the log of the noise-free output. Thus, $\rho = \log \pi_{\tilde{\theta}}(a | S_t) - \log \pi_{\theta}(a | S_t)$ captures the impact of the noise on the policy. Putting this together for the $K = 1$ case, we obtain our noise-based learning rule

$$\theta \leftarrow \theta + \eta \delta_r \epsilon^* \rho \quad (12)$$

with $\epsilon^* = \epsilon / \|\epsilon\|^2$. For convenience, we absorbed the term n into the learning rate η .

We can extend this by introducing noise into the neurons instead of the weights of the network, allowing localized perturbations within network layers. Given a layer transformation as in Equation (4), adding noise at the neuron level is represented as

$$\tilde{x}^l = f(\tilde{h}^l + \xi^l) = f(W^l \tilde{x}^{l-1} + \xi^l) \quad (13)$$

where $\xi^l \sim \mathcal{N}(0, \beta \sigma^2 I_{m^l})$ is the injected noise, β is some arbitrarily small noise scale, and m^l is the number of neurons in layer l . We use the notation \tilde{x}^l and \tilde{h}^l to denote perturbed inputs and pre-activations, respectively, which may also result from perturbations of previous network layers on which layer l depends.

To formulate the learning rule for specific layer parameters $W^l \in W$, we re-express the gradient in terms of the pre-activations instead of the parameters themselves. To do so, we first rewrite the gradient term as

$$\nabla p(W^l) = \nabla_{W^l} \log \pi_{\theta}(a | S_t) \quad (14)$$

and apply the chain rule of differentiation to break down the gradient with respect to W^l as

$$\nabla p(W^l) = \frac{\partial p}{\partial \tilde{h}^l} \frac{\partial \tilde{h}^l}{\partial W^l} = \nabla p(\tilde{h}^l) \tilde{x}^{l-1}. \quad (15)$$

Building on the theory developed above, we derive the gradient $\nabla p(\tilde{h})$, leading to the layer-specific weight update rule

$$W^l \leftarrow W^l + \eta \delta r_t \bar{\xi}^l \rho \tilde{x}^{l-1} \quad (16)$$

with $\rho = \log \pi_{\tilde{W}}(a | S_t) - \log \pi_W(a | S_t)$ and $\bar{\xi}^l = \xi^l / \|\xi^l\|^2$. Here, $\pi_{\tilde{W}}(a | S_t)$ represents the network's output when noise is injected into the neurons, while $\pi_W(a | S_t)$ corresponds to the output of the noiseless network.

2.2.3 Learning from sparse rewards

In our derivation above, synaptic updates occur at every time step, implying that learning signals and rewards are received continuously. However, rewards are usually provided after completing a sequence of actions or upon reaching specific milestones, leading to more sparsely spaced feedback. To handle this scenario, we modify our learning rule to accommodate sparse rewards arriving at arbitrary times.

Starting from Equation (9), we redefine the synaptic weight update to include time explicitly

$$W_{t+1}^l = W_t^l + \eta \delta r_t \bar{\xi}_t^l p_t \tilde{x}_t^{l-1} \quad (17)$$

where $p_t = \log \pi_{\tilde{W}}(a | S_t) - \log \pi_W(a | S_t)$. Next, we assume sparse rewards arriving at arbitrary times τ , and thus synaptic updates only occur at this moment, denoted by W_{τ}^l . The learning rule now accumulates information since the last reward was received, updating weights by integrating this information over time

$$W_{\tau}^l \leftarrow W_{\tau_0}^l + \eta \delta r_{\tau} \sum_{t=\tau_0}^{\tau} \bar{\xi}_t^l p_t \tilde{x}_t^{l-1} \quad (18)$$

where τ_0 represents the time when the previous reward was obtained.

We further represent this accumulated sum using an eligibility trace, which captures the history of neural activity and noise contributions since the last reward, defined as

$$e_{\tau} = \sum_{t=\tau_0}^{\tau} \bar{\xi}_t^l p_t \tilde{x}_t^{l-1}. \quad (19)$$

such that (18) may be expressed as

$$W_\tau^l \leftarrow W_{\tau_0}^l + \eta \delta r_\tau e_\tau. \quad (20)$$

Thus, our final learning rule consists of two primary components: (i) an eligibility trace, defined in Equation (19), which accumulates local information over time at each time step, and (ii) a synaptic update, defined in Equation (20), triggered upon reward receipt, which modulates the eligibility trace to adjust the synaptic weights.

Eligibility traces act as a mechanism to connect past actions with future rewards [19]. They capture neural activity and other local variables over time, signaling potential synaptic changes. Upon receiving a reward, these traces are modulated by the reinforcement signal, resulting in synaptic updates. Some models view eligibility traces as decaying cumulative activity [21, 48]), while others treat them as a full activity history [32], which aligns with our formulation. The eligibility trace efficiently tracks neural information between rewards, facilitating the assignment of credit to past actions.

2.3 Neural network setup

At the core of the agent’s learning and decision-making process, we use a feedforward neural network with L layers, where the transformation applied to each hidden layer is given by

$$\tilde{x}^l = f(W^l \tilde{x}^{l-1} + \xi^l) \quad (21)$$

and the readout in the output layer is given by

$$\tilde{y} = s(W^l \tilde{x}^{l-1} + \xi^l) \quad (22)$$

where a^l and x^l denote the layer pre-activation and output (with x_0 as the network input), y is the network output, $\xi^l \sim \mathcal{N}(0, \beta\sigma^2 I_{m^l})$ is noise added to the neurons, with m^l representing the number of units in layer l . This is referred to as a “noisy pass”. The function $f(\cdot)$ represents a non-linear activation function applied to each layer. In our case, we use the LeakyReLU activation function such that $f(x) = x$ if $x \geq 0$ and $f(x) = \alpha x$ with $0 < \alpha \ll 1$, otherwise. The function $s(\cdot)$ represents a softmax transformation $s_i(x) = e^{x_i} / \sum_{j=1}^{m^l} e^{x_j}$, converting the network’s output into action probabilities. We also define a “clean pass,” where no noise is present in the network, as

$$x^l = f(W^l x^{l-1}) \quad (23)$$

$$y = s(W^l x^{l-1}) \quad (24)$$

2.4 Experimental validation

We validate our approach across various environments and compare its performance with established baselines. Each environment presents an episodic problem, where the agent’s learning is guided solely by positive or negative rewards. We test in both instantaneous and delayed reward settings. In the delayed reward setting, a single reward is given after a sequence of actions, challenging the agent to assign credit retrospectively. For the instantaneous reward setting, we use the Reaching problem [18], while the delayed reward setting uses the Cartpole [1] and Acrobot [47] problems. We use implementations given by the libraries OpenAI Gym [3] and NeuroGym [33] for the different environments.

We compare NRL to two baselines: an exact-gradient version of NRL (similar to an actor-only variant of actor-critic which relies on a running average of past rewards as the prediction error), which serves as an “optimal performance” benchmark and an RMHL approach. The first baseline uses BP for gradient computation, updating eligibility traces as

$$e_\tau = \sum_{t=\tau_0}^{\tau} \nabla_W \log \pi_W(a | S_t) \quad (25)$$

The second baseline, motivated by the noise-based nature of NRL, is the RMHL rule from [26] with an explicit-noise approximation – the original version where noise is inferred from neural activities

proved too unstable for the problems considered here. For delayed rewards, we adapt it similarly to [32], updating eligibility traces as

$$e_\tau = \sum_{t=\tau_0}^{\tau} \xi_t^l \tilde{x}_t^{l-1}. \quad (26)$$

In environments with high reward variability, like Cartpole and Acrobot, we stabilize synaptic updates by scaling the RPE by dividing by r_τ . Hyperparameter values and training details are provided in Appendix B. All experiments are implemented in Python using PyTorch [37]. Our models and scripts are available for reproducibility at <https://github.com/jesusgf96/noise-based-reward-modulated-learning>.

3 Results

3.1 Solving instantaneous and delayed reward problems

To ensure comparability with RMHL methods, which typically utilize single-hidden-layer networks, we first conduct experiments with a one-hidden-layer neural network for BP, NRL, and RMHL. Training details are provided in Appendix B. In Section 3.2, we extend the comparison to deeper networks with multiple hidden layers.

First, the Reaching problem [18], visualized in Figure 1C, is an instantaneous reward problem that requires an agent to reach and stay at a target on a 1D ring by moving left, right, or staying still. At each step, the agent observes both the target’s position and its own, and it is rewarded based on its proximity to the target over fixed-duration trials. Average across-trial and final performance (mean of the last 50 trials) are shown in Figures 1A and 1B, respectively.

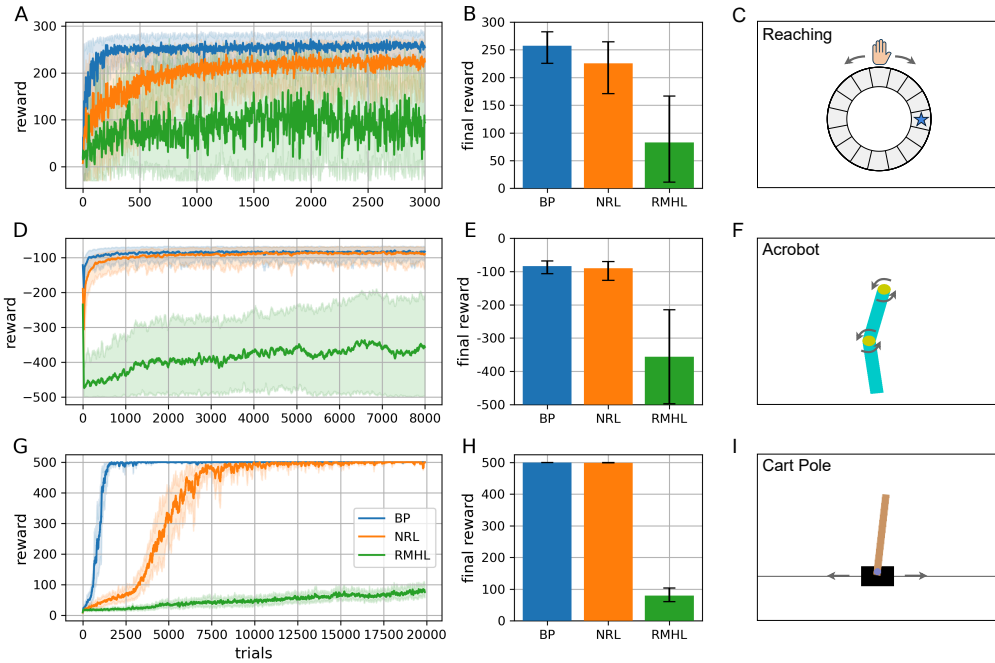


Figure 1: **Performance on benchmarks.** A, B, C: Reaching problem. D, E, F: Acrobot problem. G, H, I: Cartpole problem. Left panels: Performance across trials averaged over 5 runs. Centre panels: Final performance (mean of the last 50 trials), averaged over 5 runs. Right panels: Problem visualization.

Second, the Acrobot problem [47], visualized in Figure 1F, involves delayed reward and requires controlling a two-link robotic arm to reach a target height. At each time step, the agent observes

the angles and angular velocities of the two links and chooses one action: clockwise torque, counter-clockwise torque, or no torque. Rewards are based on the speed of completion, with a maximum time. Average across-trial and final performance (mean of the last 50 trials) are shown in Figures 1D and 1E, respectively.

The third and most challenging problem, the Cartpole problem [1], visualized in Figure 1I, is a delayed reward problem where an agent must balance a pole on a cart by moving left or right. At each time step, the agent observes the cart’s position and velocity, along with the pole’s angle and angular velocity, and acts accordingly. Performance is measured by the time the pole remains balanced, with a maximum time. Average across-trial and final performance (mean of the last 50 trials) are shown in Figures 1G and 1H, respectively.

For all three tasks, we can observe that NRL reaches the performance level of BP whereas RMHL fails to do so.

3.2 Scalability to deeper networks

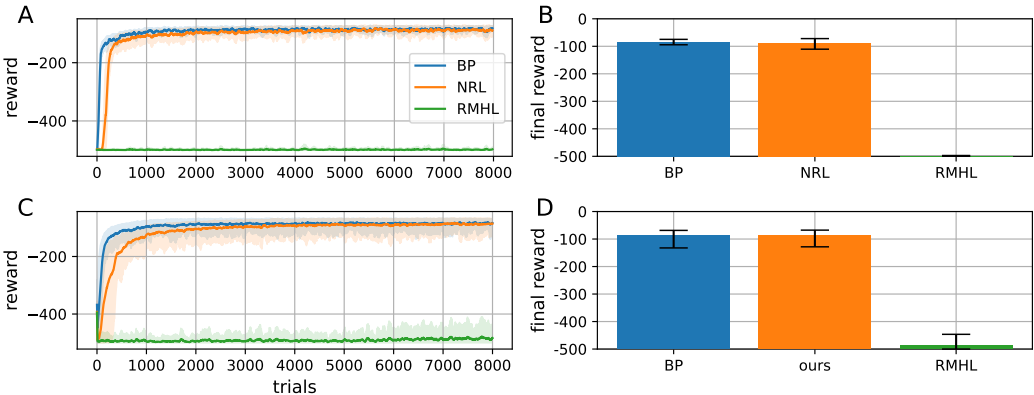


Figure 2: **Performance on deeper networks – Acrobot.** A, B: 2-hidden layer networks. C, D: 3-hidden layer networks. Left panels: Performance across trials averaged over 5 runs. Right panels: Final performance (mean of the last 50 trials), averaged over 5 runs.

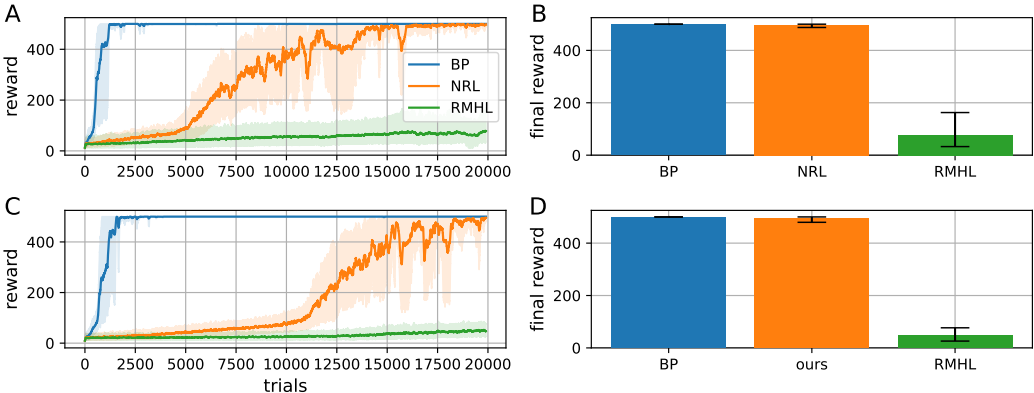


Figure 3: **Performance on deeper networks – Cartpole.** A, B: 2-hidden layer networks. C, D: 3-hidden layer networks. Left panels: Performance across trials averaged over 5 runs. Right panels: Final performance (mean of the last 50 trials), averaged over 5 runs.

Here, we demonstrate that NRL can effectively assign credit in neural networks with multiple hidden layers – a challenging scenario where most biologically plausible algorithms struggle. We use both the Acrobot and the Cartpole tasks for this purpose, as they present a delayed reward

problem, making them a more realistic test for credit assignment in reinforcement learning. In this comparison, we include the same baselines, BP and RMHL. Figure 2 displays the results for the Acrobot task and Figure 3 displays the results for the Cartpole tasks. The left panels of these two figures show performance across trials, averaged over 5 runs. In contrast, the right panels display the final performance (mean of the last 50 trials), also averaged over 5 runs. The results for neural networks with two hidden layers are shown in Figures 2A and B, and 3A and B, and those for networks with three hidden layers are presented in Figures 2C and D, and 3C and D.

Our results indicate that NRL successfully learns to solve the tasks, achieving performance comparable to BP. In contrast, RMHL struggles with credit assignment in deeper networks. However, NRL requires more trials to converge as the network depth increases—an expected outcome due to the stochastic nature of the updates [20]. A similar trend is observed with BP, though to a lesser extent, as its gradient-based updates inherently provide more directed adjustments.

3.3 Using only noisy passes

In NRL, p_t is calculated as the difference in the network’s output between the clean and noisy passes. However, a completely noiseless network is not feasible in more biophysically realistic scenarios. Instead, the clean network’s output can be approximated by averaging the outputs from multiple noisy passes, as the injected noise averages to zero over time $\lim_{N \rightarrow \infty} \frac{1}{N} \sum_{i=1}^N \xi_i^l = 0$. This assumes that the network dynamics are faster than the environment dynamics, allowing the network to perform multiple forward passes before the environment changes.

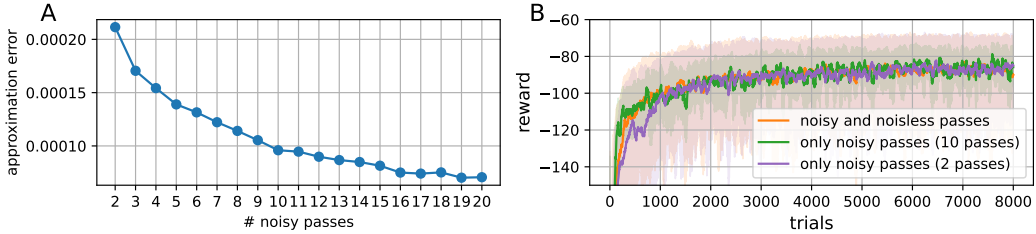


Figure 4: **Learning using only noisy passes – Acrobot.** A: Clean pass approximation error. Each data point is computed with an absolute error, averaged over 500 timesteps using the Acrobot problem. B: Acrobot problem. Performance across trials, averaged over 5 runs, with mean, minimum, and maximum values displayed.

To evaluate the accuracy of this approximation, we employ a single hidden-layer network and the Acrobot problem. The difference between the clean pass output and the averaged noisy passes output was calculated for each timestep and averaged over 500 timesteps, as shown in Figure 4A. Furthermore, Figure 4B illustrates the performance on the Acrobot problem using only noisy forward passes, starting with the minimum of 2 noisy passes. We also extended this evaluation to 10 noisy passes to explore the impact of increasing the number of passes, showing slightly faster initial convergence.

4 Discussion

In this work, we introduced NRL as a novel noise-driven learning mechanism for neural networks that bridges RL principles with Hebbian-like updates, providing a gradient-free alternative to traditional approaches. By leveraging directional derivatives and stochastic noisy neurons to approximate gradients [44, 53, 52], our method produces local synaptic updates that are modulated by a global reinforcement signal. This noise-based rule offers an efficient approach for neural adaptation, particularly suited to real-time and resource-limited environments.

NRL shares similarities with node perturbation methods [15, 20, 54, 52, 13], which inject noise into neurons to adjust weights based on state and performance fluctuations. However, unlike node perturbation—which requires constant feedback or reward for learning—NRL is well-suited for delayed-reward setups, a common scenario in real-world applications. By leveraging eligibility traces [19], NRL

can effectively assign credit to past neural states even when actions and outcomes are separated in time.

Furthermore, NRL shares conceptual similarities with forward gradient methods [2], which also estimate gradients using directional derivatives, stochastic perturbations, and forward-mode differentiation. Both frameworks leverage noise-driven updates, focusing on solving real-world tasks. However, while forward gradient methods rely solely on random perturbations to approximate gradients, NRL refines updates by incorporating reinforcement learning principles, using RPEs to directly modulate synaptic weights. Recent advances in forward gradient techniques, such as employing local auxiliary networks to produce informed gradient guesses [16], have demonstrated substantial improvements in alignment with exact gradients, narrowing the performance gap with backpropagation. Similarly, these variance-reduction strategies could inspire further refinements in our approach, enhancing the quality of noise-based updates and improving scalability to more complex architectures.

Another increasingly popular approach for gradient estimation during optimization is zeroth-order (ZO) optimization [28, 6]. Like NRL, common ZO optimization relies on perturbation-driven strategies, utilizing differences in function values resulting from input perturbations to approximate gradients. However, as with forward gradient methods, NRL distinguishes itself by incorporating elements, such as RPEs and eligibility traces, to learn in delayed reward scenarios. Unlike forward gradient methods, which rely on directional derivatives and access to the model’s structure, ZO methods estimate gradients purely from function evaluations, without requiring any knowledge of the network’s internal structure or differentiability. This makes ZO methods particularly well-suited for black-box optimization tasks, a flexibility that our approach also shares.

The results demonstrate the effectiveness of NRL, significantly outperforming the comparable RMHL approach [26, 32] in both instantaneous and delayed reward tasks. While RMHL methods aim to align neural dynamics with observed brain dynamics rather than optimizing learning, our learning rule is rigorously derived to perform gradient approximation. As a result, our learning rule introduces two key innovations. First, normalizing the noise, $\bar{\xi}_t^l = \xi_t^l / \|\xi_t^l\|^2$, allows for smaller noise magnitudes that minimally impact agent behavior while still contributing effectively to the learning process. Second, an additional term, $p_t = [\log \pi_{\bar{g}}(a|S_t) - \log \pi_{\theta}(a|S_t)]$, captures the influence of noise on the network output, thereby enhancing credit assignment accuracy.

Our results further demonstrate that NRL effectively assigns credit even in deep networks with multiple hidden layers, a challenge for many biologically plausible algorithms. As network depth increases, NRL’s performance advantage over RMHL becomes more pronounced. In fact, RMHL struggles with credit assignment in networks with more than one hidden layer, as evidenced by its minimal performance improvements during training. Nevertheless, NRL does require more trials to converge in deeper networks, which is an expected consequence of its stochastic update mechanism [20].

Compared to traditional BP-based methods, NRL approximates gradients rather than relying on exact gradients [27, 51, 39, 38], offering a significant advantage in computationally constrained scenarios—such as when using non-differentiable networks like spiking neural networks [55, 50]. The local-update structure of NRL provides compatibility with neuromorphic hardware [42], where efficient, low-power computations are essential. Neuromorphic systems can also inherently simulate noisy neural activity, enabling energy-efficient learning in applications where real-time adaptation is key.

The inherent noise in NRL is also advantageous for RL, as it naturally facilitates exploration-exploitation balance [22, 25]. Injected noise perturbs neural states, promoting exploratory deviations from expected values and thus introducing variations in the agent’s policy.

Our work further draws inspiration from neuroscience and underscores the importance of biologically plausible approaches [56, 30] for advancing learning algorithms. The reliance on RPEs as learning signals emulates the dopaminergic reward signals observed in the brain [41, 40], crucial for synaptic plasticity. The noise-based rule, coupled with eligibility traces, also aligns with biological processes that enable learning under uncertainty [14] and reflect the noisy nature of the brain [9, 45, 31]. Notice that the definition of RPEs used in this work is a simplification, relying on a straightforward running average for reward prediction. While this is sufficient to capture the core ideas of the proposed learning mechanism, more sophisticated approaches could further enhance reward estimation. One such extension is Temporal Difference (TD) learning [46, 48], which provides a more principled method for predicting expected future rewards and aligns more closely with biological dopaminergic activity [35]. A natural implementation would be an actor-critic architecture, where a critic network estimates the

value function (e.g., expected future rewards), refining the reward prediction error (RPE).

One limitation of NRL is its dependence on multiple forward passes per synaptic update, which, though parallelizable, reduces biological plausibility. Future work could explore efficient ways to estimate noise impacts without explicitly needing separate clean and noisy passes. Additionally, while BP may offer faster convergence in unrestricted computational settings, recent research, including this study and others [7, 11], show promise in bridging this gap for specific networks and tasks.

Our findings suggest that noise-based learning strategies could drive advances in machine learning by enabling efficient, local, and energy-conscious algorithms, particularly suited for neuromorphic hardware and real-time applications. This research also offers valuable insights into how learning might occur in the brain, enriching our understanding of both artificial and biological intelligence.

Acknowledgments

This publication is part of the DBI2 project (024.005.022, Gravitation), which is financed by the Dutch Ministry of Education (OCW) via the Dutch Research Council (NWO).

References

- [1] Andrew G Barto, Richard S Sutton, and Charles W Anderson. Neuronlike adaptive elements that can solve difficult learning control problems. *IEEE Transactions on Systems, Man, and Cybernetics*, (5):834–846, 1983.
- [2] Atılım Güneş Baydin, Barak A Pearlmutter, Don Syme, Frank Wood, and Philip Torr. Gradients without backpropagation. *arXiv preprint arXiv:2202.08587*, 2022.
- [3] Greg Brockman, Vicki Cheung, Ludwig Pettersson, Jonas Schneider, John Schulman, Jie Tang, and Wojciech Zaremba. Openai gym. arxiv. *arXiv preprint arXiv:1606.01540*, 10, 2016.
- [4] Jeroen Burms, Ken Caluwaerts, and Joni Dambre. Reward-modulated hebbian plasticity as leverage for partially embodied control in compliant robotics. *Frontiers in Neurorobotics*, 9:9, 2015.
- [5] Gert Cauwenberghs. A fast stochastic error-descent algorithm for supervised learning and optimization. *Advances in Neural Information Processing Systems*, 5, 1992.
- [6] Aochuan Chen, Yimeng Zhang, Jinghan Jia, James Diffenderfer, Jiancheng Liu, Konstantinos Parasyris, Yihua Zhang, Zheng Zhang, Bhavya Kailkhura, and Sijia Liu. Deepzero: Scaling up zeroth-order optimization for deep model training. *arXiv preprint arXiv:2310.02025*, 2023.
- [7] Sander Dalm, Marcel van Gerven, and Nasir Ahmad. Effective learning with node perturbation in deep neural networks. *arXiv preprint arXiv:2310.00965*, 2023.
- [8] Amir Dembo and Thomas Kailath. Model-free distributed learning. *IEEE Transactions on Neural Networks*, 1(1):58–70, 1990.
- [9] A Aldo Faisal, Luc PJ Selen, and Daniel M Wolpert. Noise in the nervous system. *Nature Reviews Neuroscience*, 9(4):292–303, 2008.
- [10] Jesús García Fernández, Nasir Ahmad, and Marcel Van Gerven. Ornstein-Uhlenbeck adaptation as a mechanism for learning in brains and machines. *Entropy*, 26:1125, 2024.
- [11] Jesús García Fernández, Sander Keemink, and Marcel van Gerven. Gradient-free training of recurrent neural networks using random perturbations. *Frontiers in Neuroscience*, 18:1439155, 2024.
- [12] Silvia Ferrari, Bhavesh Mehta, Gianluca Di Muro, Antonius MJ VanDongen, and Craig Henriquez. Biologically realizable reward-modulated hebbian training for spiking neural networks. In *2008 IEEE International Joint Conference on Neural Networks (IEEE World Congress on Computational Intelligence)*, pages 1780–1786. IEEE, 2008.

- [13] Ila R Fiete and H Sebastian Seung. Gradient learning in spiking neural networks by dynamic perturbation of conductances. *Physical Review Letters*, 97(4):048104, 2006.
- [14] József Fiser, Pietro Berkes, Gergő Orbán, and Máté Lengyel. Statistically optimal perception and learning: from behavior to neural representations. *Trends in Cognitive Sciences*, 14(3):119–130, 2010.
- [15] Barry Flower and Marwan Jabri. Summed weight neuron perturbation: An $O(n)$ improvement over weight perturbation. *Advances in Neural Information Processing Systems*, 5, 1992.
- [16] Louis Fournier, Stéphane Rivaud, Eugene Belilovsky, Michael Eickenberg, and Edouard Oyallon. Can forward gradient match backpropagation? In *International Conference on Machine Learning*, pages 10249–10264. PMLR, 2023.
- [17] Nicolas Frémaux and Wulfram Gerstner. Neuromodulated spike-timing-dependent plasticity, and theory of three-factor learning rules. *Frontiers in Neural Circuits*, 9:85, 2016.
- [18] Apostolos P Georgopoulos, Andrew B Schwartz, and Ronald E Kettner. Neuronal population coding of movement direction. *Science*, 233(4771):1416–1419, 1986.
- [19] Wulfram Gerstner, Marco Lehmann, Vasiliki Liakoni, Dane Corneil, and Johanni Brea. Eligibility traces and plasticity on behavioral time scales: experimental support of neohebbian three-factor learning rules. *Frontiers in Neural Circuits*, 12:53, 2018.
- [20] Naoki Hiratani, Yash Mehta, Timothy Lillicrap, and Peter E Latham. On the stability and scalability of node perturbation learning. *Advances in Neural Information Processing Systems*, 35:31929–31941, 2022.
- [21] Eugene M Izhikevich. Solving the distal reward problem through linkage of stdp and dopamine signaling. *Cerebral Cortex*, 17(10):2443–2452, 2007.
- [22] Leslie Pack Kaelbling, Michael L Littman, and Andrew W Moore. Reinforcement learning: A survey. *Journal of Artificial Intelligence Research*, 4:237–285, 1996.
- [23] Yuji Kawai and Minoru Asada. Spatiotemporal motor learning with reward-modulated hebbian plasticity in modular reservoir computing. *Neurocomputing*, 558:126740, 2023.
- [24] Łukasz Kuśmierz, Takuya Isomura, and Taro Toyozumi. Learning with three factors: modulating hebbian plasticity with errors. *Current Opinion in Neurobiology*, 46:170–177, 2017.
- [25] Pawel Ladosz, Lilian Weng, Minwoo Kim, and Hyondong Oh. Exploration in deep reinforcement learning: A survey. *Information Fusion*, 85:1–22, 2022.
- [26] Robert Legenstein, Steven M Chase, Andrew B Schwartz, and Wolfgang Maass. A reward-modulated hebbian learning rule can explain experimentally observed network reorganization in a brain control task. *Journal of Neuroscience*, 30(25):8400–8410, 2010.
- [27] Seppo Linnainmaa. The representation of the cumulative rounding error of an algorithm as a Taylor expansion of the local rounding errors. *Master’s Thesis (in Finnish), Univ. Helsinki*, pages 6–7, 1970.
- [28] Sijia Liu, Pin-Yu Chen, Bhavya Kailkhura, Gaoyuan Zhang, Alfred O Hero III, and Pramod K Varshney. A primer on zeroth-order optimization in signal processing and machine learning: Principals, recent advances, and applications. *IEEE Signal Processing Magazine*, 37(5):43–54, 2020.
- [29] Wolfgang Maass. Noise as a resource for computation and learning in networks of spiking neurons. *Proceedings of the IEEE*, 102(5):860–880, 2014.
- [30] Adam H Marblestone, Greg Wayne, and Konrad P Kording. Toward an integration of deep learning and neuroscience. *Frontiers in Computational Neuroscience*, 10:215943, 2016.

- [31] Mark D McDonnell and Lawrence M Ward. The benefits of noise in neural systems: bridging theory and experiment. *Nature Reviews Neuroscience*, 12(7):415–425, 2011.
- [32] Thomas Miconi. Biologically plausible learning in recurrent neural networks reproduces neural dynamics observed during cognitive tasks. *Elife*, 6:e20899, 2017.
- [33] Manuel Molano-Mazon, Joao Barbosa, Jordi Pastor-Ciurana, Marta Fradera, Ru-Yuan Zhang, Jeremy Forest, Jorge del Pozo Lerida, Li Ji-An, Christopher J Cueva, Jaime de la Rocha, et al. Neurogym: An open resource for developing and sharing neuroscience tasks. *PsyArXiv*, 2022.
- [34] P Read Montague, Peter Dayan, and Terrence J Sejnowski. A framework for mesencephalic dopamine systems based on predictive hebbian learning. *Journal of Neuroscience*, 16(5):1936–1947, 1996.
- [35] Yael Niv. Reinforcement learning in the brain. *Journal of Mathematical Psychology*, 53(3):139–154, 2009.
- [36] John P O’Doherty, Jeffrey Cockburn, and Wolfgang M Pauli. Learning, reward, and decision making. *Annual Review of Psychology*, 68(1):73–100, 2017.
- [37] Adam Paszke, Sam Gross, Francisco Massa, Adam Lerer, James Bradbury, Gregory Chanan, Trevor Killeen, Zeming Lin, Natalia Gimelshein, Luca Antiga, et al. Pytorch: An imperative style, high-performance deep learning library. *Advances in Neural Information Processing Systems*, 32, 2019.
- [38] Sebastian Ruder. An overview of gradient descent optimization algorithms. *arXiv preprint arXiv:1609.04747*, 2016.
- [39] David E Rumelhart, Geoffrey E Hinton, and Ronald J Williams. Learning internal representations by error propagation. Technical report, California Univ San Diego La Jolla Inst for Cognitive Science, 1985.
- [40] Wolfram Schultz. Dopamine reward prediction error coding. *Dialogues in Clinical Neuroscience*, 18(1):23–32, 2016.
- [41] Wolfram Schultz, Peter Dayan, and P Read Montague. A neural substrate of prediction and reward. *Science*, 275(5306):1593–1599, 1997.
- [42] Catherine D Schuman, Shruti R Kulkarni, Maryam Parsa, J Parker Mitchell, Bill Kay, et al. Opportunities for neuromorphic computing algorithms and applications. *Nature Computational Science*, 2(1):10–19, 2022.
- [43] H Sebastian Seung. Learning in spiking neural networks by reinforcement of stochastic synaptic transmission. *Neuron*, 40(6):1063–1073, 2003.
- [44] James C Spall. Multivariate stochastic approximation using a simultaneous perturbation gradient approximation. *IEEE Transactions on Automatic Control*, 37(3):332–341, 1992.
- [45] Richard B Stein, E Roderich Gossen, and Kelvin E Jones. Neuronal variability: noise or part of the signal? *Nature Reviews Neuroscience*, 6(5):389–397, 2005.
- [46] Richard S Sutton. Learning to predict by the methods of temporal differences. *Machine Learning*, 3:9–44, 1988.
- [47] Richard S Sutton. Generalization in reinforcement learning: Successful examples using sparse coarse coding. *Advances in Neural Information Processing Systems*, 8, 1995.
- [48] Richard S Sutton. Reinforcement learning: An introduction. *A Bradford Book*, 2018.
- [49] Richard S Sutton, David McAllester, Satinder Singh, and Yishay Mansour. Policy gradient methods for reinforcement learning with function approximation. *Advances in Neural Information Processing Systems*, 12, 1999.

- [50] Amirhossein Tavanaei, Masoud Ghodrati, Saeed Reza Kheradpisheh, Timothée Masquelier, and Anthony Maida. Deep learning in spiking neural networks. *Neural Networks*, 111:47–63, 2019.
- [51] P Werbos. *Beyond Regression: New Tools for Prediction and Analysis in the Behavioral Sciences*. PhD thesis, 1974.
- [52] Justin Werfel, Xiaohui Xie, and H Seung. Learning curves for stochastic gradient descent in linear feedforward networks. *Advances in Neural Information Processing Systems*, 16, 2003.
- [53] Bernard Widrow and Michael A Lehr. 30 years of adaptive neural networks: perceptron, madaline, and backpropagation. *Proceedings of the IEEE*, 78(9):1415–1442, 1990.
- [54] Ronald J Williams. Simple statistical gradient-following algorithms for connectionist reinforcement learning. *Machine Learning*, 8:229–256, 1992.
- [55] Kashu Yamazaki, Viet-Khoa Vo-Ho, Darshan Bulsara, and Ngan Le. Spiking neural networks and their applications: A review. *Brain Sciences*, 12(7):863, 2022.
- [56] Anthony Zador, Sean Escola, Blake Richards, Bence Ölveczky, Yoshua Bengio, Kwabena Boahen, Matthew Botvinick, Dmitri Chklovskii, Anne Churchland, Claudia Clopath, et al. Catalyzing next-generation artificial intelligence through neuroai. *Nature Communications*, 14(1):1597, 2023.
- [57] Paul Züge, Christian Klos, and Raoul-Martin Memmesheimer. Weight versus node perturbation learning in temporally extended tasks: Weight perturbation often performs similarly or better. *Physical Review X*, 13(2):021006, 2023.

A Gradient approximation using directional derivatives

Consider a function $f(\theta)$, where $\theta = (W_1, \dots, W_L)$ are its parameters. The gradient of this function is defined as follows:

Definition A.1. *The gradient ∇f is a vector indicating the direction of the steepest ascent of the function f , with components as partial derivatives of $f(\theta)$:*

$$\nabla f = \left[\frac{\partial f}{\partial \theta} \right]^\top = \left[\frac{\partial f}{\partial W_1}, \dots, \frac{\partial f}{\partial W_L} \right]^\top. \quad (27)$$

While ∇f captures the rate of change of f in the steepest direction, a directional derivative gives the rate of change in a specified direction. For a unit vector $v = \epsilon / \|\epsilon\|$, normalized via the Euclidean norm, we define the directional derivative as:

Definition A.2. *The directional derivative of $f(\theta)$ along a unit vector $v = (v_1, \dots, v_n)$ is defined by the limit*

$$\nabla_v f(\theta) = \lim_{h \rightarrow 0} \frac{f(\theta + hv) - f(\theta)}{h}, \quad (28)$$

where h is a small step size.

For a sufficiently small h we approximate the directional derivative as

$$\nabla_v f(\theta) = \frac{f(\theta + h\epsilon) - f(\theta)}{h\|\epsilon\|}. \quad (29)$$

This directional derivative is essentially a projection of ∇f in the direction v , following the relation:

$$\nabla_v f(\theta) = v \cdot \nabla f(\theta). \quad (30)$$

We can now formally demonstrate how gradients can be approximated using directional derivatives.

Theorem A.3. *Let $\epsilon \sim \mathcal{N}(0, \sigma^2 I_n)$, drawn from some probability distribution $p(\epsilon)$, and n the number of dimensions in θ . Exact gradients can be written in terms of directional derivatives using expectations*

$$\nabla f(\theta) = n \mathbb{E}_{p(\epsilon)} [v \nabla_v f(\theta)^\top]. \quad (31)$$

Proof.

$$\begin{aligned} \nabla f(\theta) &= n \mathbb{E}_{p(\epsilon)} [v \nabla_v f(\theta)^\top] \\ &= n \mathbb{E}_{p(\epsilon)} [v v \nabla f(\theta)^\top] \\ &= n \mathbb{E}_{p(\epsilon)} [v v] \nabla f(\theta)^\top \\ &= n \mathbb{E}_{p(\epsilon)} \left[\frac{\epsilon}{\|\epsilon\|} \frac{\epsilon^\top}{\|\epsilon\|} \right] \nabla f(\theta) \\ &= n \frac{1}{n} I_n \nabla f(\theta) = \nabla f(\theta) \end{aligned}$$

as we assume $p(\epsilon) = \mathcal{N}(0, \sigma^2 I_n)$, which gives $\mathbb{E}[v v^\top] = \mathbb{E} \left[\frac{\epsilon}{\|\epsilon\|} \frac{\epsilon^\top}{\|\epsilon\|} \right] = \frac{1}{n} I_n$. \square

Now, consider gradient descent in the direction of the gradient $\nabla f(\theta)$ as

$$\theta_{t+1} = \theta_t + \alpha \nabla f(\theta_t). \quad (32)$$

This update can be reformulated using directional derivatives.

Theorem A.4. *Let $\eta = \alpha n$ and $\epsilon^{(i)} \sim \mathcal{N}(0, \sigma^2 I_n)$. Gradient descent is equivalent to the update rule*

$$\theta_{t+1} = \theta_t + \alpha \sum_{i=1}^K \left[\frac{\epsilon^{(i)}}{\|\epsilon^{(i)}\|^2} \left[f(\theta + \epsilon^{(i)}) - f(\theta) \right]^\top \right] \quad (33)$$

in the limit when $\sigma^2 \rightarrow 0$ and $K \rightarrow \infty$.

Proof.

$$\begin{aligned}
\nabla f(\theta) &= n\mathbb{E}_{p(\epsilon)} [v\nabla_v f(\theta)^\top] \\
&= n\mathbb{E}_{p(\epsilon)} \left[v \left[\frac{f(\theta + h\epsilon) - f(\theta)}{h\|\epsilon\|} \right]^\top \right] \\
&= n\mathbb{E}_{p(\epsilon)} \left[\frac{\epsilon}{\|\epsilon\|} \left[\frac{f(\theta + h\epsilon) - f(\theta)}{h\|\epsilon\|} \right]^\top \right]
\end{aligned}$$

Assuming a small h and σ^2 , we can absorb $1/h$ into the learning rate and h into the variance σ^2 .

$$\nabla f(\theta) = n\mathbb{E}_{p(\epsilon)} \left[\frac{\epsilon}{\|\epsilon\|^2} [f(\theta + \epsilon) - f(\theta)]^\top \right]$$

We may approximate the expectation by sampling under some empirical distribution to obtain

$$\nabla f(\theta) = n \sum_{i=1}^K \left[\frac{\epsilon^{(i)}}{\|\epsilon^{(i)}\|^2} [f(\theta + \epsilon^{(i)}) - f(\theta)]^\top \right]$$

□

In practice, sufficiently small σ^2 and limited noise samples approximate the gradient. For $K = 1$, analogous to single-sample updates in stochastic gradient descent:

$$\theta_{t+1} = \theta_t + \eta \frac{\epsilon}{\|\epsilon\|^2} \delta f \tag{34}$$

with $\delta f = [f(\theta + \epsilon) - f(\theta)]^\top$.

B Model hyperparameters and training details

All hyperparameters were carefully tuned per method and problem to ensure fair comparisons across methods. The number of episodes was chosen to illustrate the convergence of our method relative to baseline methods, with 8000, 20000, and 1000 episodes used for the Acrobot, Cartpole, and Reaching problems, respectively. In all our experiments, we set the smoothing factor for reward estimation to $\lambda = 0.66$, striking a balance between recent values (for quick adaptability) and a longer history (for robustness against rapid reward fluctuations). Each neural network consisted of an input, hidden, and output layer. Input units corresponded to environment observation elements, and output units to possible actions. Specifically, Acrobot, Cartpole, and Reaching used 6, 4, and 32 input units and 3, 2, and 2 output units, respectively, with hidden layer sizes of 64, 64, and 128. Table 1 summarizes the learning rate η and noise standard deviation σ for each method and problem. Higher values of these parameters could lead to unstable training, while lower values may result in slower learning.

Table 1: Learning rate η and noise standard deviation σ for the different learning algorithms across problems. Dashes indicate that the parameter is not used.

		BP	Ours	RMHL
Acrobot	η	5e-3	5e-2	5e-2
	σ	-	1e-3	1e-3
Cartpole	η	5e-3	5e-2	1e-2
	σ	-	1e-3	1e-1
Reaching	η	1e-2	1e-2	1e-1
	σ	-	1e-3	1e-1